Bandwidth analysis of waveguide grating coupler

Xiao, Zhe; Liow, Tsung-Yang; Zhang, Jing; Shum, Perry Ping; Luan, Feng

2013

Xiao, Z., Liow, T. Y., Zhang, J., Shum, P., & Luan, F. (2013). Bandwidth analysis of waveguide grating coupler. Optics Express, 21(5), 5688-5700.

https://hdl.handle.net/10356/96434

https://doi.org/10.1364/OE.21.005688

Bandwidth analysis of waveguide grating coupler

Zhe Xiao,[1,2] Tsung-Yang Liow,[2] Jing Zhang,[4] Ping Shum,[1,3] and Feng Luan[1,3,*]

[1]*OPTIMUS, School of Electrical and Electronics Engineering, Nanyang Technological University, Singapore 639798*
[2]*Institute of Microelectronics, Agency for Science, Technology and Research (A*STAR), 11 Science Park Road, Science Park II, Singapore 117685*
[3]*CINTRA CNRS/NTU/THALES, UMI 3288, Research Techno Plaza, 50 Nanyang Drive, Singapore 639798*
[4]*National Metrology Centre, A*STAR, 1 Science Park Drive, Singapore 118221*
**LuanFeng@ntu.edu.sg*

Abstract: The bandwidth of planar waveguide grating couplers is theoretically investigated based on the rigorous grating theory. We observe that the bandwidth behavior is not only determined by the grating coupler intrinsic properties, but also affected by the fiber parameters such as position, beam waist and Numerical Aperture. The rigorous bandwidth formula is derived. By analyzing the formula, several practical guidelines are proposed for grating coupler design and fiber operation in order to achieve wideband performance.

OCIS codes: (050.1950) Diffraction gratings; (130.0130) Integrated optics.

References and links

1. M. Hochberg and T. Baehr-Jones, "Towards fabless silicon photonics," Nat. Photonics **4**(8), 492–494 (2010).
2. F. Van Laere, G. Roelkens, M. Ayre, J. Schrauwen, D. Taillaert, D. Van Thourhout, T. F. Krauss, and R. Baets, "Compact and highly efficient grating couplers between optical fiber and nanophotonic Waveguides," J. Lightwave Technol. **25**(1), 151–156 (2007).
3. I. A. Avrutsky, A. S. Svakhin, V. A. Sychugov, and O. Parriaux, "High-efficiency single-order waveguide grating coupler," Opt. Lett. **15**(24), 1446–1448 (1990).
4. X. Chen, C. Li, C. K. Y. Fung, S. M. G. Lo, and H. K. Tsang, "Apodized waveguide grating couplers for efficient coupling to optical fibers," IEEE Photon. Technol. Lett. **22**(15), 1156–1158 (2010).
5. G. Roelkens, D. Van Thourhout, and R. Baets, "High efficiency silicon-on-Insulator grating coupler based on a poly-silicon overlay," Opt. Express **14**(24), 11622–11630 (2006).
6. C. R. Doerr, L. Chen, Y. Chen, and L. L. Buhl, "Wide bandwidth silicon nitride grating coupler," IEEE Photon. Technol. Lett. **22**(19), 1461–1463 (2010).
7. X. Chen, K. Xu, Z. Cheng, C. K. Y. Fung, and H. K. Tsang, "Wideband subwavelength gratings for coupling between silicon-on-insulator waveguides and optical fibers," Opt. Lett. **37**(17), 3483–3485 (2012).
8. Z. Xiao, F. Luan, T. Y. Liow, J. Zhang, and P. Shum, "Design for broadband high-efficiency grating couplers," Opt. Lett. **37**(4), 530–532 (2012).
9. T. Tamir, "Beam and waveguide couplers," in *Integrated Optics* (Springer, 1975).
10. T. K. Gaylord and M. G. Moharam, "Analysis and applications of optical diffraction by gratings," Proc. IEEE **73**(5), 894–937 (1985).
11. R. G. Hunsperger, *Integrated Optics: Theory and Technology* (Springer, 2008).
12. J. C. Brazas and L. Li, "Analysis of input-grating couplers having finite lengths," Appl. Opt. **34**(19), 3786–3792 (1995).
13. D. Taillaert, F. Van Laere, M. Ayre, W. Bogaerts, D. Van Thourhout, P. Bienstman, and R. Baets, "Grating couplers for coupling between optical fibers and nanophotonic waveguides," Jpn. J. Appl. Phys. **45**(8A), 6071–6077 (2006).
14. T. Tamir and S. T. Peng, "Analysis and Design of Grating Couplers," Appl. Phys. (Berl.) **14**(3), 235–254 (1977).
15. S. T. Peng, T. Tamir, and H. L. Bertoni, "Theory of periodic dielectric waveguides," IEEE Trans. Microw. Theory Tech. **23**(1), 123–133 (1975).
16. S. Miyanaga and T. Asakura, "Intensity profile of outgoing beams from uniform and linearly tapered grating couplers," Appl. Opt. **20**(4), 688–695 (1981).

1. Introduction

Silicon photonic devices are promising for various optical processing on a dense integrated photonic chip fabricated by CMOS compatible technology [1]. Diffraction grating couplers provide a practical and effective means of light coupling between fiber and chip. They are

#178770 - $15.00 USD Received 26 Oct 2012; revised 14 Nov 2012; accepted 20 Nov 2012; published 1 Mar 2013

easier to package in a monolithic system and capable of multi-port applications. Efficiency and bandwidth are two critical specifications of planar waveguide grating couplers. While many novel techniques, such as adding bottom reflection mirror [2, 3], apodized grating strength [4] and polysilicon overlay [5], were proposed to increase the coupling efficiency, only a few attempts have been reported to increase the coupling bandwidth. C. R. Doerr et.al first made an approximate calculation of the bandwidth of grating couplers by relating the efficiency drop in the coupling spectrum to the wavelength-dependent diffraction angles [6]. This approach overestimates the coupling bandwidth, as the grating dispersion effects have been neglected. Based on the same understanding, X. Chen et.al gave a supplemental discussion with the grating dispersion effects being considered [7]. We gave a different explanation on the bandwidth issue, attributing the coupling bandwidth to the mismatch of effective indices between the diffracted beam and the actual grating structure around the resonance wavelength [8], which more directly reveals the intrinsic bandwidth mechanism of grating couplers. However, all these aforementioned studies are only based on simple estimations rather than rigorous derivation. Especially, the 1 dB bandwidth coefficient introduced as a constant in these bandwidth approximations has no proper physics explanation, which is too rough that important details are ignored. In this paper, we derive the rigorous bandwidth formula for planar waveguide grating couplers based on the rigorous grating theory [9]. We find that the 1 dB coefficient is not a constant value but a function of both fiber parameters such as beam waist and position and the grating parameters such as the field decay rate of the grating coupler etc. We investigate in detail the effect of each of these parameters on the bandwidth behavior. A complete analysis is presented based on the rigorous bandwidth formula, which offers new insights on grating bandwidth and also provides practical guidelines for grating design and fiber operation for wideband fiber-to-chip excitation. In the later discussion, the content is arranged as follows: In section 2, we start from the fiber-to-chip input coupling to derive the rigorous bandwidth formula. As a verification of the formula, the analytic results are compared with the FDTD simulation and reported experimental results for several grating couplers of different structures; in section 3, the effect of individual parameter on bandwidth performance is separately investigated, and an intuitive physics explanation is then given based on the results; owing to reciprocality of fiber-to-chip grating coupling system, the bandwidth formula is also adapt for the chip-to-fiber output coupling, in section 4, we will discuss and explain the rigorous bandwidth formula for the output coupling case. Finally, as a summary, several useful guidelines are presented for grating design and fiber operation.

2. Derivation of rigorous bandwidth formula for fiber-to-chip excitation

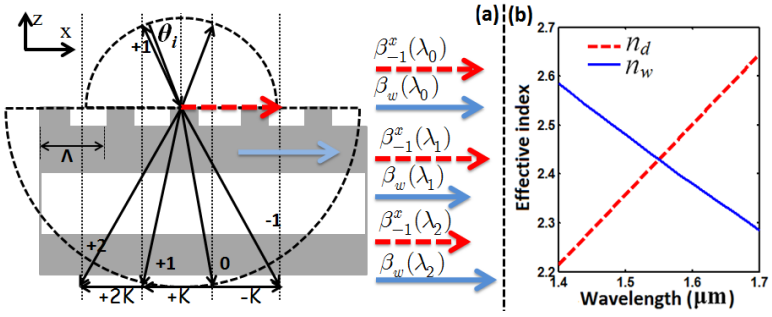

Fig. 1. (a) Grating coupler model for fiber to waveguide excitation and wavevector diagram (Wave expansion with wavevector from vector Floquet Condition [10]); (b) dispersion diagram.

In this section, we first give a brief introduction of the coupling principle for a fiber-to-chip grating system, and an intuitive explanation is presented on the bandwidth mechanism. The theoretical model of a planar waveguide grating coupler is shown in Fig. 1(a). Here the

#178770 - $15.00 USD Received 26 Oct 2012; revised 14 Nov 2012; accepted 20 Nov 2012; published 1 Mar 2013

rigorous wave expansion from vector Floquet condition is adopted for wavevector illustration. There are other completely equivalent rigorous wave expansions given in [10], these expansions have different wavevector magnitudes in z axis but their tangential component are completely the same along the grating surface. While optical beam is incident into grating coupler from the fiber at tilt angle θ_i, the interaction of the grating in redirecting the incident light is simply dividing the incident light into many diffracted inhomogeneous plane waves that have directions given by $\beta_q = \beta_u - q\mathrm{K}$, where $q = 0, \pm 1, \pm 2,...$, q is the diffracted order number, β_u is the wavevector of the undiffracted beam (i.e. $q = 0$), and β_q is the wavevector of the q diffracted order. K is grating vector, which is defined as $\mathrm{K} = 2\pi/\Lambda_0$. This condition is known as Floquet condition [10], which indicates the satisfaction of boundary conditions for tangential electric field along the periodic grating surface. Each order of the diffracted lights is determined by the incident field (the undiffracted item β_u) and the grating structure (qK item). In Fig. 1, the −1 order diffracted light is illustrated for fiber to waveguide coupling as it is used in most practical grating couplers (−1 order is also considered in the following discussion). When coupling occurs, it is required that the tangential phase velocity of −1 order diffracted wave is able to be the same with that of the guided mode in the grating region for the guided mode excitation [11]. Consider the case without grating structure, a fundamental problem is encountered that the phase velocity of the refractive light is always smaller than the guided mode of the waveguide along the propagation direction, causing that the guided mode cannot be excited. The grating therefore serves as enabling to match the phase velocity with the guided mode by −1 order diffracted light in the grating region. According to the coupling theory, the strongest coupling occurs while the diffracted light has the same tangential wavevector with the guided mode of the grating coupler. However, since the wavevectors of the diffracted light and guided mode are functions of wavelength with different slopes, so only one intersection exists in the dispersion diagram (here $\lambda - n_{eff}$ diagram is utilized). By taking silicon grating coupler as an example, Fig. 1(b) illustrates the typical dispersion diagram for grating couplers, where n_w is the effective index of guided mode in the grating region and n_d is index of diffracted light. A more intuitive illustration is given in Fig. 1(a), the wavevectors of the diffracted light and the guided mode are well-matched at resonance wavelength λ_0 for the strongest coupling, but at other wavelength that deviating from the resonance wavelength (like $\lambda_1 > \lambda_0$ or $\lambda_2 < \lambda_0$ in Fig. 1(a)), a mismatch is introduced between both wavevectors which is attributed to the drop in coupling efficiency. Based on the Floquet condition, the wavevector mismatch can be written as:

$$\Delta\beta = \beta_w - \beta_{-1}^x = \frac{2\pi}{\lambda} n_w - \left(\frac{2\pi}{\lambda} n_0 \sin\theta_i + \frac{2\pi}{\Lambda_0}\right) \tag{1}$$

where n_0 is the refractive index of top cladding, β_w is the wavevector of the guide mode, β^x_{-1} is the tangential wavevector of the −1 order diffracted light, n_w is the effective index of the grating region, θ_i is the incident angle and Λ_0 is the grating pitch. Using the Taylor series expansion of Eq. (1) at the resonance wavelength λ_0 with the condition of $\Delta\beta(\lambda_0) = 0$ and keeping the first order term of $\Delta\lambda$ (here we write in form of absolute value), we obtain:

$$\Delta\beta = \pm\frac{2\pi}{\lambda_0}|\Delta\lambda| \cdot \left| \frac{1}{\Lambda_0} - \frac{dn_w(\lambda)}{d\lambda}\Big|_{\lambda=\lambda_0} \right| \tag{2}$$

In Eq. (2), the positive sign is for the wavelength range of $\lambda < \lambda_0$, the negative sign is for $\lambda > \lambda_0$. Now we investigate the effect of such a mismatch on the coupling bandwidth based on rigorous grating theory [9]. Figure 2 schematically illustrates a typical grating coupler interface in the coordinates. The coordinate origin (x = 0) is located at the first pitch of the gratings. The amplitude distribution of the fiber beam can be modeled by a Gaussian profile shown in Fig. 2. Provided that the x-axis position of the beam center is at $-d$. The field amplitude of the fiber

#178770 - $15.00 USD Received 26 Oct 2012; revised 14 Nov 2012; accepted 20 Nov 2012; published 1 Mar 2013

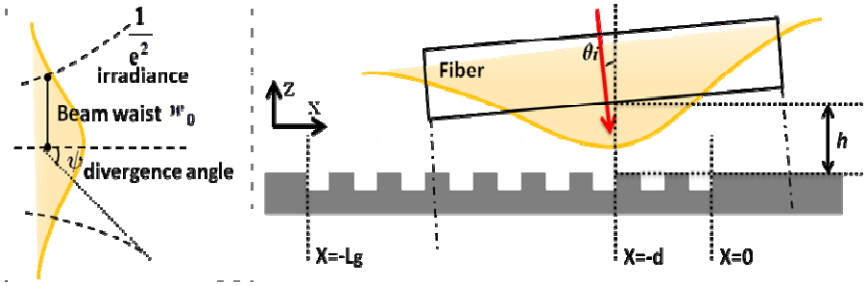

Fig. 2. Fiber Gaussian beam model and schematic grating coupler structure in coordination system.

beam can be expressed as (E_0 indicates the peak amplitude):

$$s_0(x) = E_0 \cdot e^{-(x+d)^2/w_0^2} \tag{3}$$

The incident fiber beam propagates along z axis with a tilt angle θ_i. Then, the amplitude distribution of the beam impinging on the grating coupler surface can be approximated by:

$$\begin{cases} s(x) = E_0 \cdot e^{-(x+d)^2/w_1^2} \\ w_1 \simeq [w_0 + h\tan(\psi)]/\cos(\theta_i) \end{cases} \tag{4}$$

where h is the height between the fiber and grating surface shown in Fig. 2(w_0 is much greater than h), ψ is the divergence angle of the Gaussian fiber beam, w_1 can be also expressed as:

$$w_1 \simeq [w_0 + h\frac{\mathrm{NA}}{n_0\cos(\psi)}]/\cos(\theta_i) \tag{5}$$

In order to calculate the coupling efficiency, the complex amplitude of the guided wave in the grating region excited by the fiber source (precisely, in the fiber beam effectively covered grating region) is expressed as $A(x) = a(x)\cdot e^{i\beta_w x}$. Thus, the coupling efficiency is given by:

$$\eta = C\cdot|a(0)|^2 \tag{6}$$

where C is a constant, $a(x)$ is the reduced field amplitude in the grating region, which is determined by three contributions: the amplitude decay rate α due to grating diffraction, the external fiber source distribution, $s(x)$, and the wavevector mismatch, $_{\Delta\beta}$. It should be noted that, for the input-coupling, the diffracted inhomogeneous plane wave in the grating region has a tangential wavevector $\beta_{-1}^x = \beta_w - \Delta\beta$, so $a(x)$ has a factor of $e^{-(\alpha+\Delta\beta i)x}$. The reduced field amplitude $a(x)$ therefore satisfies the differential equation [9, 12]:

$$\frac{da(x)}{dx} = -(\alpha + i\Delta\beta)a(x) + c\cdot s(x) \tag{7}$$

Based on Eq. (6) into Eq. (7), the solution of the coupling efficiency can be written as Eq. (8), of which we make the integral operation over the grating area in [-L_g, 0], and the final expression of the coupling efficiency is given by Eq. (9).

$$\eta = C'\left|\int_{-Lg}^{0} e^{(\alpha+i\Delta\beta)x} e^{-(x+d)^2/w_1^2}\,dx\right|^2 \tag{8}$$

#178770 - $15.00 USD Received 26 Oct 2012; revised 14 Nov 2012; accepted 20 Nov 2012; published 1 Mar 2013

$$\begin{cases} \eta = \dfrac{1}{4} C' \pi w_1^2 e^{\frac{1}{2}(-4\alpha d + \alpha^2 w_1^2 - \Delta\beta^2 w_1^2)} \cdot C_{erf} \\ C_{erf} = \left| -Erf[-\dfrac{d}{w_1} + \dfrac{1}{2}(\alpha + \Delta\beta i) w_1] + Erf[\dfrac{-d + L_g}{w_1} + \dfrac{1}{2}(\alpha + \Delta\beta i) w_1] \right|^2 \end{cases} \tag{9}$$

C' is a constant coefficient by integral. The coupling efficiency calculated using Eq. (9) is the absolute efficiency, in order to examine the efficiency drop caused by the wavevector mismatch $\Delta\beta$, we define the normalized efficiency referring to the zero detuning as below:

$$\eta_0 = \frac{\eta}{\eta\big|_{\Delta\beta=0}} = e^{-\frac{1}{2}\Delta\beta^2 w_1^2} \cdot \frac{C_{erf}}{C_{erf}\big|_{\Delta\beta=0}} \tag{10}$$

Consider 1 dB normalized efficiency in Eq. (10), ie, $\eta_0 = 10^{-0.1}$ and based on the relationship between the wavelength deviation $\Delta\lambda$ and the wavevector mismatch $\Delta\beta$ given by Eq. (2), we can obtain the corresponding wavelength deviation $\Delta\lambda_{1dB}$ that resulting in 1 dB efficiency drop given by Eq. (11). It is worth to mention that $\Delta\lambda_{1dB}$ indicates the wavelength variation for 1 dB efficiency drop at each side of the resonance wavelength, which should be calculated separately for both regions (i.e. for both cases of $\Delta\beta > 0$ and $\Delta\beta < 0$, or say, for the corresponding wavelength region $\lambda < \lambda_0$ and $\lambda > \lambda_0$). In the discussion below, we call $\Delta\lambda_{1dB}$ as 1 dB wavelength variation.

$$\begin{cases} \Delta\lambda_{1dB} = \dfrac{1}{\left| \dfrac{1}{\Lambda_0} - \dfrac{dn_w(\lambda_0)}{d\lambda} \right|} \cdot C_{1dB} \\ C_{1dB} = \dfrac{\lambda_0}{2\pi w_1} \sqrt{\dfrac{ln10}{5} + 2ln \dfrac{C_{erf}}{C_{erf}\big|_{\Delta\beta=0}}} \end{cases} \tag{11}$$

By substituting Eq. (5) into Eq. (11), $\Delta\lambda_{1dB}$ can be related to fiber numerical aperture and divergence angle given by:

$$\Delta\lambda_{1dB} = \frac{1}{\left| \dfrac{1}{\Lambda_0} - \dfrac{dn_w(\lambda_0)}{d\lambda} \right|} \cdot \frac{n_0 \cos(\theta_i) \cdot \lambda_0}{2\pi[w_0 n_0 + h \cdot \mathrm{NA}/\cos(\psi)]} \sqrt{\frac{ln10}{5} + 2ln \frac{C_{erf}}{C_{erf}\big|_{\Delta\beta=0}}} \tag{12}$$

$$\mathrm{NA} = n_0 \sin\psi \approx \lambda_0 / \pi w_0 \tag{13}$$

Using Eq. (13), we can also write the rigorous bandwidth formula in other equivalent form. Compared Eq. (11) and Eq. (12) to the bandwidth formulas in references [7] and [8], we find that the 1 dB bandwidth coefficient introduced in these references should not be a constant, which is actually determined by both the fiber and grating parameters. We will analyze these parameters in detail in later section. Here several gating couplers are taken as examples to discuss the bandwidth calculation using the derived rigorous bandwidth formula. The analytic results will be compared with the FDTD calculation and reported experimental results for verification. In Table 1, C-I is a silicon grating coupler with a ploy-silicon overlay [5], and it works at TE polarization. C-II is conventional TE grating silicon coupler with shallow etching depth [13]. C-III is a horizontal slot waveguide grating coupler for TM mode excitation proposed in [8]. C-IV is a 400 nm silicon nitride grating coupler which has fully etched structure with pitch of 1.14 μm and filling factor of 50%. While BOX layer thickness is tuned

#178770 - $15.00 USD Received 26 Oct 2012; revised 14 Nov 2012; accepted 20 Nov 2012; published 1 Mar 2013

to 2.2 μm, the best efficiency of 45% is achievable. The main parameters required for calculation include the grating dispersion at resonance wavelength, grating pitch Λ_0, amplitude decay rate α, fiber x-axis position d and waist w_0. Note that here the fiber position d is optimized for the best efficiency in these references as it is used in practical cases. Grating dispersion can be easily obtained by mode field analysis. With FDTD technique, through observing the mode field decay of the guided mode propagating in the core layer of the grating region, α value can be obtained. It is worth to mention that α is the field amplitude decay, i.e. half of the decay rate in intensity. α is determined by the grating parameters such as the etching depth etc. The intensity decay profiles for the three grating couplers C-I, C-II, C-III and C-IV are illustrated in Figs. 2(a), 2(c), 2(e) and 2(g), respectively. The intensity decay factors are calculated by fitting the exponent coefficient indicated in Fig. 3. Utilizing the parameters listed in Table 1, we can plot the two curves determined by Eq. (2) and Eq. (11) to calculate the 1 dB bandwidth for the three grating couplers in Figs. 2(b), 2(d) and 2(f), respectively (The bandwidth can't be calculated solely by Eq. (11), because the 1 dB $\Delta\beta$ variation also exists in C_{1dB}). In this group of figures, two intersection points actually indicate two solutions of the equation system by Eq. (2) and Eq. (11). The ordinates of the two intersections correspond to the 1 dB wavelength variation $\Delta\lambda_{1dB}$ in the cases of $\lambda < \lambda_0$ and $\lambda > \lambda_0$, respectively. It is obvious that they have almost the same value, which can explain the nearly symmetric spectral response of grating couplers at both sides of the resonance wavelength. By summing up the wavelength variations (or approximating by doubling the $\Delta\lambda_{1dB}$), we can obtain the total 1 dB bandwidth for the three grating couplers. The bandwidth results are given in Table 1 along with the cited simulation and experimental results. We can see that the bandwidths calculated by the derived rigorous equations have a good agreement with the simulation and experimental results. Based on Figs. 2(b), 2(d), 2(f), 2(h) and Table 1, we can also observed that, for these grating couplers excited by 10μm-diameter fiber beam, the wavevector mismatch is about 0.2 for 1 dB wavelength variation while the fiber position is optimized for the best efficiency. Equations (2) and (11) reflect the intrinsic bandwidth property of grating couplers which does not include external layer factors such as the substrate, BOX layer, and top cladding. However, we also observe that while the parameters of external layers are optimized to achieve the best coupling efficiency for practical purpose, i.e. exerting constructive interferences into the grating region, then the interfaces outside the gating layers have little impact on the achievable bandwidth. Taking the substrate reflection as an example, the reflection normally has a spectrum with much wider bandwidth than the coupling bandwidth due to the short optical path difference. While the layer is tuned for constructive interference back into grating region, the peak of both spectrums will be overlapped at the resonance wavelength; because of the relatively small power of the reflection light and its large bandwidth, it has little impact on the coupling bandwidth.

#178770 - $15.00 USD Received 26 Oct 2012; revised 14 Nov 2012; accepted 20 Nov 2012; published 1 Mar 2013

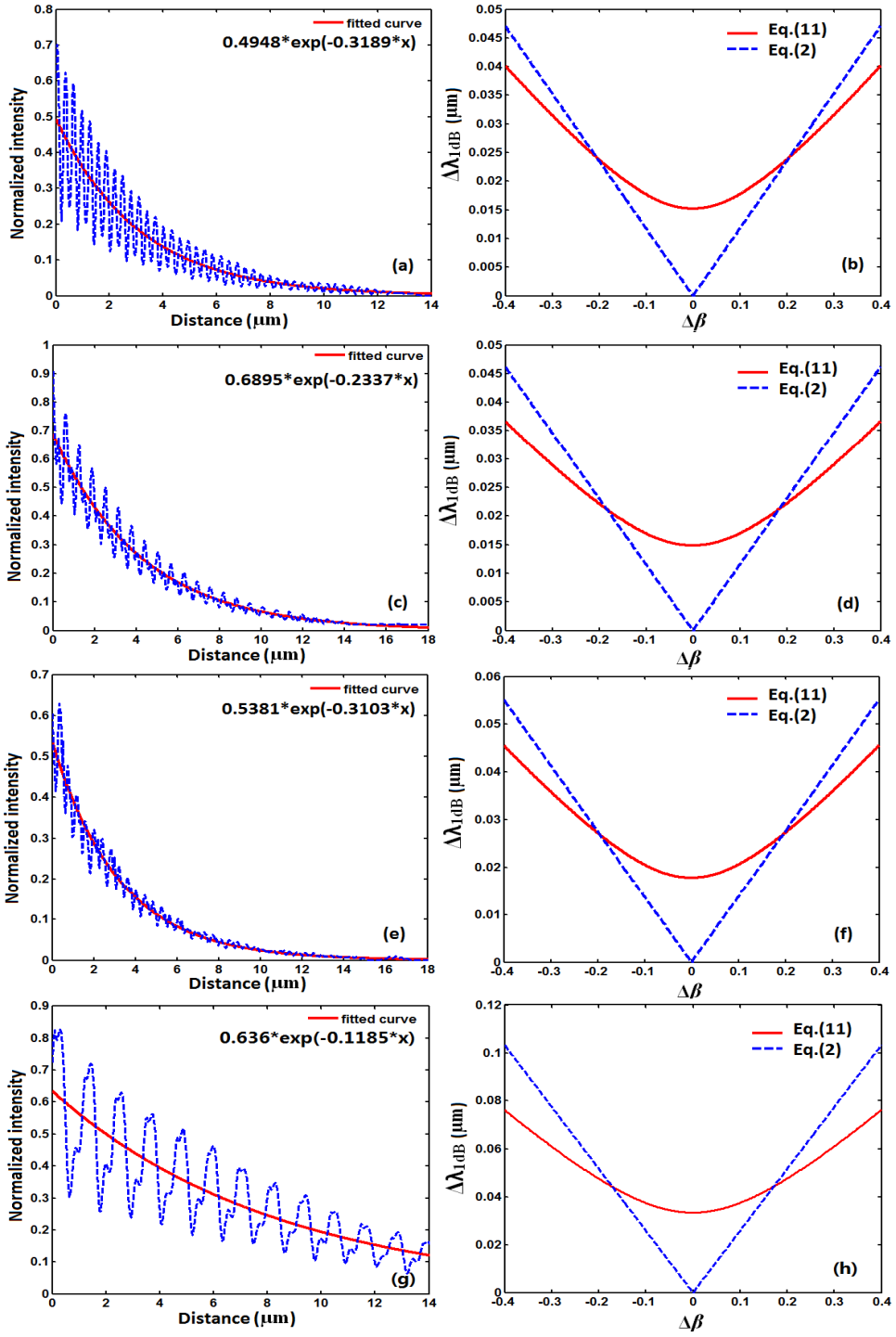

Fig. 3. Grating field decay and the bandwidth calculation by Eq. (2) and Eq. (11): (a) and (b) for C-I; (c) and (d) for C-II; (e) and (f) for C-III; (g) and (h) for C-IV.

#178770 - $15.00 USD Received 26 Oct 2012; revised 14 Nov 2012; accepted 20 Nov 2012; published 1 Mar 2013

Table 1. ***Grating parameters and bandwidth calculation by FDTD and formula***

Parameters & performance		**C-I**	**C-II**	**C-III**	**C-IV**
Grating & fiber parameters	Λ_0 (nm)	610	630	814	1140
	$dn_w(\lambda)/d\lambda$ (μm^{-1})*	–0.457	–0.55	–0.56	–0.078
	amplitude decay rate α	0.1595	0.1169	0.1552	0.0592
	fiber x position d (μm)	3.6	4.2	3.8	3.8
	incident angle θ_i	10°	10°	8°	8°
	beam waist w_0 (μm)	5.2	5.2	5.2	5.2
Bandwidth	$\Delta\lambda_{1dB}$ by FDTD calculation	50nm [5]	44nm [13]	60nm [8]	86nm
	$\Delta\lambda_{1dB}$ by experiment	50nm [5]	42nm [13]	–	–
	$\Delta\lambda_{1dB}$ by Eq. (2) and (11)	48nm	44nm	56nm	86nm
Efficiency	η_p by simulation	66% [5]	36% [13]	65% [8]	45%

3. Investigation of the effect of individual parameter on bandwidth behavior

In this section, we investigate the effect of individual parameter on bandwidth performance of planar waveguide grating couplers. We take grating coupler C-I as an example for this part discussion. Likewise, both the analytic results and FDTD calculation results are given as a comparison. In Eq. (11), the grating pitch and dispersion relationship are determined by the grating materials and structure, which are fixed after the grating design. Here, we focus on discussion of the parameters in C_{1dB} including the fiber x-axis position d, fiber beam size w_0 and amplitude decay factor α. Let us first examine the dependency of coupling bandwidth on the fiber position. Figure 4 (a) illustrates the bandwidth calculated by Eqs. (2) and (11) for a group of different fiber position values. It can be seen that the 1 dB bandwidth decreases with increase of fiber position d. The same trend is also achieved by the FDTD results shown in the inset of Fig. 4(b). The comparison of bandwidth calculation by the rigorous equations and simulation results is also illustrated in Fig. 4(b), which indicates a good agreement. The small difference (ceiling to 4 nm) of both bandwidth results comes from the calculation accuracy limitation.

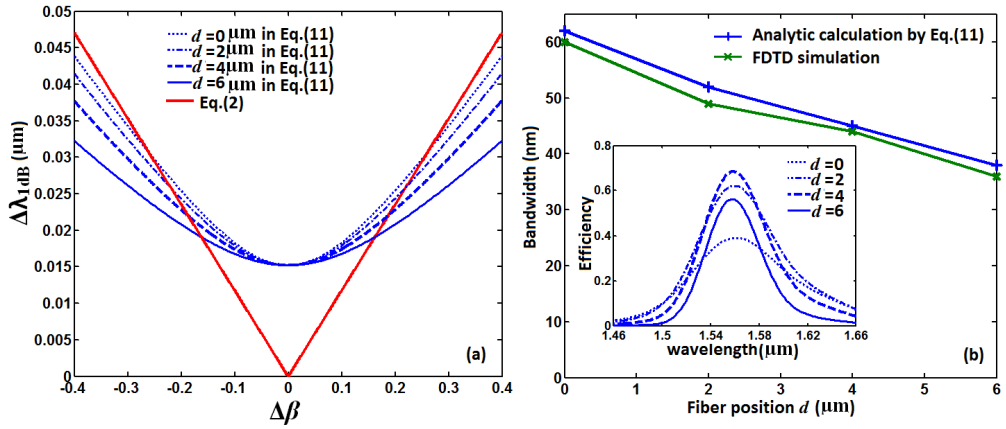

Fig. 4. (a) The analytic bandwidth calculation based on Eq. (2) and Eq. (11) for different fiber x-axis position d; (b) Comparison of the bandwidth calculation by FDTD simulation and analytic results. Inset: spectral response obtained by FDTD simulation.

#178770 - $15.00 USD Received 26 Oct 2012; revised 14 Nov 2012; accepted 20 Nov 2012; published 1 Mar 2013

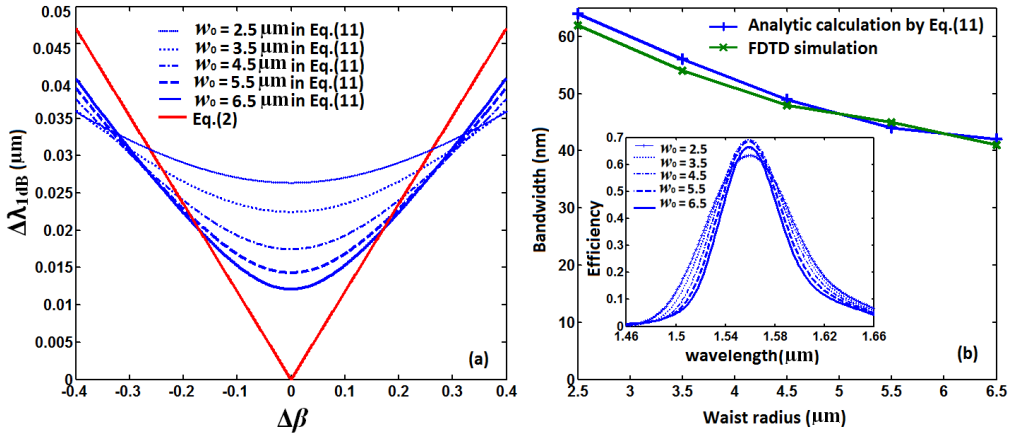

Fig. 5. (a) The analytic bandwidth calculation based on Eq. (2) and Eq. (11) for different fiber waist w_0; (b) Comparison of the bandwidth calculation by FDTD simulation and analytic results. Inset: spectral response obtained by FDTD simulation.

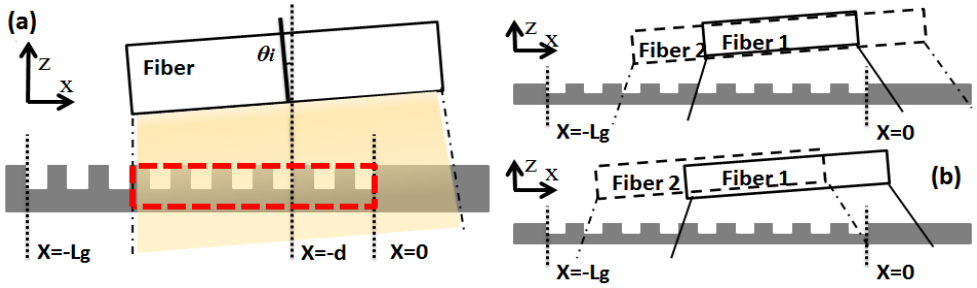

Fig. 6. The illustration of "effective interaction area" and its alteration as fibers beam waist and position changes.

Then, we investigate the effect of fiber beam waist w_0 on the coupling bandwidth. In the same way, the analytic results are illustrated in Fig. 5(a). It can be observed that the coupling bandwidth will increase when the grating is excited by a fiber beam with smaller waist. The results of FDTD calculation are given in the inset of Fig. 5(b), which verifies the trend. The comparison of 1 dB bandwidth calculated by the rigorous equations and simulation results is given in Fig. 5(b). By comparing the Fig. 4(b) and Fig. 5(b), we observe that to adjust the beam waist is a better choice to broaden the coupling bandwidth because it would not induce great efficiency drop meanwhile increasing the coupling bandwidth. In addition, according to Eq. (13), it is known that the Gaussian beam with smaller beam waist exerts a larger numerical aperture. It means that to increase the incident beam numerical aperture will also broaden the coupling bandwidth.

These relationships are directly determined by the monotonicity of the solution of Eqs. (2) and (11). The curve of Eq. (2) keeps unchanging after the grating structure is fixed. Thus, $\Delta\lambda_{1dB}$ is mainly affected by the parameters of C_{1dB} in Eq. (11). By examining the mathematic properties of C_{1dB}, we give a more intuitive explanation for these relationships. We first introduce a definition of "effective interaction area", that is, the fiber beam effectively covered grating area. In Fig. 6(a), the dash-line labeled area indicates the effective interaction area. In actuality, to alter the fiber beam waist or position is inherently changing the size of effective interaction area and power distribution in the area. Figure 6(b) intuitively illustrates the effective interaction area when fibers beam waist and position changes. It is clear that a larger beam waist or a further distance between the fiber center and the first gating pitch (x = 0) exerts a larger interaction area, which will result in narrower coupling bandwidth according to the aforementioned discussion. The trends can be simply understood that since the

#178770 - $15.00 USD Received 26 Oct 2012; revised 14 Nov 2012; accepted 20 Nov 2012; published 1 Mar 2013

wavevector mismatch always exists in the effective interaction area for the wavelengths that deviating the

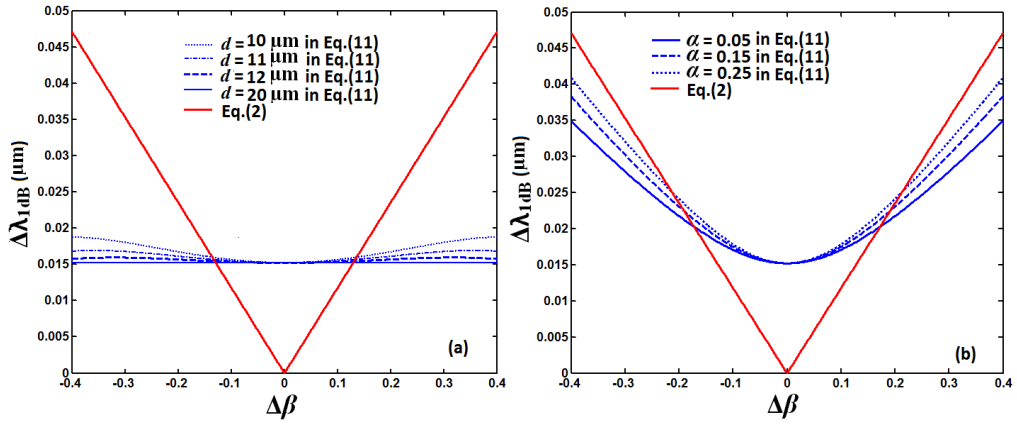

Fig. 7. (a) The analytic bandwidth calculation based on Eq. (2) and Eq. (11) for relatively large fiber position *d*;(b)The analytic bandwidth calculation for different field amplitude decay rate α

resonance wavelength λ_0, so a longer traveling distance in the area will induce more serious efficiency drop for these wavelengths and therefore narrow down the coupling bandwidth. Moreover, as stated by Eqs. (7) and (8), the reduced field amplitude $a(x)$ in the grating region has a factor of $e^{-(\alpha+\Delta\beta i)x}$, α is the field amplitude decay rate and $\Delta\beta$i can be also viewed as a decay factor. Since the integral operation needs to be done over the whole effective interaction area, a longer effective interaction area in the propagation direction therefore results in a smaller coupling bandwidth. It is easy to imagine that the size of the effective interaction area will become constant while the distance d from the first gating pitch to fiber center is large enough (larger than w_1). In Fig. 7(a), we show the bandwidth calculation for the case that the fiber is put relatively far away from the grating beginning (d equals to 10, 11, 12 and 20 μm). It can be seen that the 1 dB bandwidth is almost changeless (about 30nm) even though d keep increasing. The results are verified by FDTD simulation as well.

Finally, we investigate the relationship between the bandwidth and the field amplitude decay rate α. The value of α mainly depends on the gating materials and structure parameters such as etching depth etc. However, α is not easy to be solely adjusted because other parameters in Eq. (11) such as grating pitch and dispersion will also changes correspondingly when the gating structure changes. Here, we just simply consider the monotonicity of the bandwidth versus the field amplitude decay rate α by assuming other parameters remain unchanged. In Fig. 7(b), we change the field amplitude decay rate α with value of 0.05, 0.15 and 0.25 to calculate the 1 dB bandwidth. We can see that the bandwidth monotonically increases with the increase of α.

4. Bandwidth for waveguide to fiber excitation

Owing to reciprocality of fiber-to-chip grating coupling system, the transmission spectrum is the same for waveguide to fiber and fiber to waveguide coupling cases. The rigorous bandwidth formula can be adapted for the chip-to-fiber output coupling case. In this section, we give a brief discussion on the case of waveguide to fiber output coupling. The model of waveguide to fiber coupling is shown in Fig. 8(a).The output coupling can be described as the guided mode propagates along open periodic dielectric waveguide (grating region) [14] and the optical power gradually radiates into the claddings. The grating coupler is regarded as a structure that transforms a surface wave into one or more leaky waves (space-harmonic fields) into top cladding and BOX layer. The upward power will be partly collected by the fiber. The wavevectors of each order of space-harmonic waves are related by [14, 15]:

#178770 - $15.00 USD Received 26 Oct 2012; revised 14 Nov 2012; accepted 20 Nov 2012; published 1 Mar 2013

$$\beta_q = \beta_w + qK \tag{14}$$

where q = 0, ± 1, ± 2, ..., q is the order number, β_w is the wavevector of the guided mode in the grating structure, and β_q is the wavevector of the q order space-harmonic wave. In the tangential direction, Eq. (2.4) can be written for −1 order wave as below:

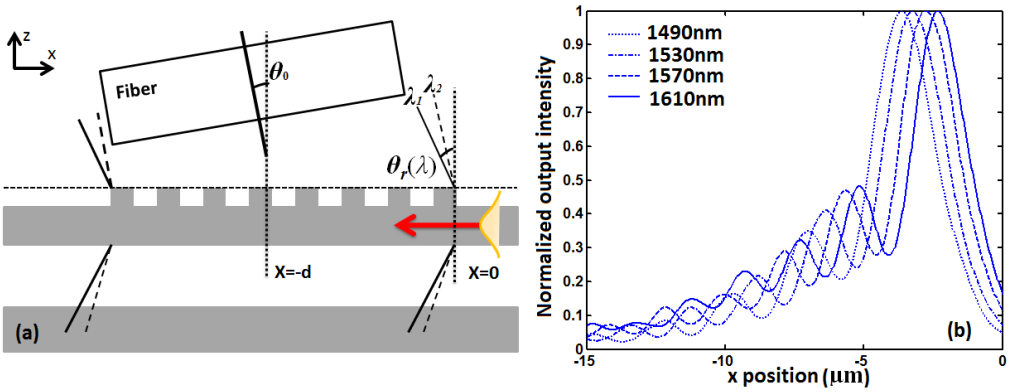

Fig. 8. (a) The model of output coupling from waveguide to fiber coupling; (b) The typical intensity profile of the output radiation waves

$$\beta_{-1}^{x} = \beta_w - \frac{2\pi}{\Lambda_0} \tag{15}$$

The corresponding expression in form of the effective index can be written as:

$$n_0 \sin\theta_r(\lambda) = n_w - \frac{\lambda}{\Lambda_0} \tag{16}$$

where n_w is the effective index of the guided mode in the grating structure. θ_r is the diffraction angle. θ_r can be viewed as a function of wavelength, that is, the radiation angle of the space-harmonic wave is wavelength dependent. Taking grating coupler C-II as an example, the output intensity profile is illustrated for several different wavelengths. It can be seen that the intensity peak shifts with different wavelength. The amplitude decay rate α is a critical parameter that determining the shape of the output profile. More details of the output intensity profile of grating couplers were theoretically investigated in [16]. Since the fiber has a tilt angle θ_0, so it can more effectively receive the radiation wave that transmitting upward at this angle. Thus, the coupling efficiency of the corresponding wavelength wave will be higher than other wavelengths, which leads to a coupling window of certain bandwidth. Based on this understanding, the bandwidth of grating coupler may be approximated by relating the 1 dB wavelength variation to the derivative of θ_r. In previous work, the bandwidth formula for the output coupling is derived by introducing a constant 1 dB coefficient as (note that in this paper, $\Delta\lambda_{1\mathrm{dB}}$ means 1 dB wavelength variation instead of the total 1 dB bandwidth) [7]:

$$\Delta\lambda_{1dB} = \frac{n_0 \cos(\theta_0)}{\left|\frac{1}{\Lambda_0} - \frac{dn_w(\lambda_0)}{d\lambda}\right|} \cdot \eta_{1\mathrm{dB}} \tag{17}$$

Comparing Eq. (17) with Eq. (12), we can find that both the formulas have the similar form, and the bandwidth coefficient can be expressed as:

#178770 - $15.00 USD Received 26 Oct 2012; revised 14 Nov 2012; accepted 20 Nov 2012; published 1 Mar 2013

$$\eta_{1\mathrm{dB}} = \frac{\lambda_0}{2\pi[w_0 n_0 + h \cdot \mathrm{NA}/\cos(\psi)]} \sqrt{\frac{In10}{5} + 2In \frac{C_{erf}}{C_{erf}\big|_{\Delta\beta=0}}} \tag{18}$$

Likewise, $\eta_{1\mathrm{dB}}$ is a function of fiber and grating parameters including d, w_0 and α (NA and divergence angle ψ are directly determined by the fiber beam waist w_0 according to Eq. (13)). The monotonicity of the rigorous bandwidth formula has been investigated in section 2 for the input coupling case. Here, we give an intuitive explanation on these monotonic relationships for the output coupling case. As stated for the input coupling case, we know that increasing the fiber x-axis position d and beam waist w_0 will decrease the coupling bandwidth owing to a larger effective interaction area. Similarly, for the output coupling case, we can define an "effective collection area" at the fiber butt. The amount of receiving power can be calculated through integral of the Pointing vector over this area. Thus, a larger effective collection area of the fiber will increase the difference in collecting efficiency between the radiation wave of the best accepting wavelength (ie. the wave transmitting upward right at the fiber tilt angle) and other wavelengths, and therefore leads to a narrower coupling bandwidth. Obviously, to increase the fiber x-axis position and beam waist are the means to increase the effective collection area. In addition, as for the amplitude decay rate α in the coefficient $\eta_{1\mathrm{dB}}$, it is known that the shape of the output intensity profile also affect the coupling performance; α will affect the output intensity profile [16] and thus influence the bandwidth behavior. The monotonicity of the coupling bandwidth versus the field amplitude decay rate α has been discussed in section 3 for the input coupling case.

5. Summary and guidelines for grating coupler design and fiber operation

In summary, we have derived the rigorous bandwidth formula for planar waveguide grating couplers. The coupling bandwidth is determined by the grating coupler intrinsic properties and also affected by the fiber parameters such as position and beam waist etc. We investigated the effect of individual parameter on bandwidth behavior and obtained some intuitive vision on the bandwidth behavior of grating couplers. Based on the previous works [6–8] as well as discussion in this paper, we summarize and list some useful guidelines for grating coupler design and fiber operation for broad bandwidth performance as follows: Firstly, in order to design wideband grating coupler, we should attempt to make gratings pitch as large as possible by decreasing the refractive index of the grating area. This can be achieved by adopting relatively low refractive index materials (silicon nitride) or through perturbation of the grating groove in lateral direction or using refractive index engineering structures etc. However, in view of the coupling efficiency, to decrease the refractive index of the grating area normally leads to a lower refractive index contrast with the claddings in the grating region, which therefore makes the incident light easily travel through the structure and leak into the claddings. Hence, with this approach, we should consider controlling the power leakage to the claddings during the design. Secondly, according to the bandwidth formula, to properly design the grating structure (or choose special materials) of smaller dispersion can also increase the coupling bandwidth. As for the fiber operation, the basic idea of broadening the coupling bandwidth is to reduce the effective interaction grating area. This can be achieved by putting the fiber closer to the grating start or using a fiber with smaller beam waist or a larger numerical aperture. To optimize the beam size (or numerical aperture) is a better choice because it would not induce great efficiency drop (if the beam size is not greatly squeezed) meanwhile increasing the coupling bandwidth. Larger amplitude decay rate α in the grating region will also increase the coupling bandwidth, but α is usually difficult to be solely adjusted in real operation. The derived formula cannot be directly applied to calculate the bandwidth of apodized grating couplers or the grating couplers with non-uniform period. However, the basic principles given in our paper are still useful to analyze non-uniform gratings which can be viewed as many very short pieces of uniform gratings with different properties. In this case, the change of the grating property along propagation direction can be expressed as Δβ as a function of x. Following the same analysis given in this paper, we can

#178770 - $15.00 USD Received 26 Oct 2012; revised 14 Nov 2012; accepted 20 Nov 2012; published 1 Mar 2013

find a more general formula that covers the non-uniform cases. Another factor that can affect the bandwidth is the beam profile. In our derivation, Gaussian beam is adopted to model the incident beam from single mode fiber. The further study can be considered to vary the beam patterns (ie. to modify the s(x) item in Eq. (7)) to increase the coupling bandwidth meanwhile remaining high coupling efficiency. Overall, grating couplers are critical in optical system as the practical interface between fiber-link and nanophotonic structures, large bandwidth can bring better fabrication and operation tolerance and it is required for some wideband applications such as high speed optical communication.

Acknowledgments

This work was supported in part by the Nanyang Technological University (NTU) under Grant NTU-SUG-M4080142 MOE RG24/10 and in part by the Institute of Microelectronics, Agency for Science, Technology and Research (A*STAR) Science and Engineering Research Council under Grant 1021290052.

#178770 - $15.00 USD Received 26 Oct 2012; revised 14 Nov 2012; accepted 20 Nov 2012; published 1 Mar 2013